

# Analyses of cell death mechanisms related to amino acid substitution at position 95 in the rabies virus matrix protein

Isshu Kojima<sup>1,2</sup>, Fumiki Izumi<sup>3</sup>, Makoto Ozawa<sup>1,2,4</sup>, Yoshikazu Fujimoto<sup>1,2</sup>, Misuzu Okajima<sup>1,2</sup>, Naoto Ito<sup>3,5</sup>, Makoto Sugiyama<sup>3,5</sup> and Tatsunori Masatani<sup>1,2,3,5,\*</sup>

## Abstract

We previously reported that the avirulent fixed rabies virus strain Ni-CE induces a clear cytopathic effect in mouse neuroblastoma cells, whereas its virulent progenitor, the Nishigahara strain, does not. Infection with Nishigahara and Ni-CE mutants containing a single amino acid substitution in the matrix protein (M) demonstrated that the amino acid at position 95 of M (M95) is a cytopathic determinant. The characteristics of cell death induced by Ni-CE infection resemble those of apoptosis (rounded and shrunken cells, DNA fragmentation), but the intracellular signalling pathway for this process has not been fully investigated. In this study, we aimed to elucidate the mechanism by which M95 affects cell death induced by human neuroblastoma cell infection with the Nishigahara, Ni-CE and M95-mutated strains. We demonstrated that the Ni-CE strain induced DNA fragmentation, cell membrane disruption, exposure of phosphatidylserine (PS), activation of caspase-3/7 and anti-poly (ADP-ribose) polymerase 1 (PARP-1) cleavage, an early apoptosis indicator, whereas the Nishigahara strain did not induce DNA fragmentation, caspase-3/7 activation, cell membrane disruption, or PARP-1 cleavage, but did induce PS exposure. We also demonstrated that these characteristics were associated with M95 using M95-mutated strains. However, we found that Ni-CE induced cell death despite the presence of a caspase inhibitor, Z-VAD-FMK. In conclusion, our data suggest that M95 mutation-related cell death is caused by both the caspase-dependent and -independent pathways.

## INTRODUCTION

Rabies virus (RABV) causes lethal neurological symptoms in mammals and has a mortality rate of almost 100%. There is no effective cure for rabies and effective vaccines are not widely available, resulting in an estimated 59000 human deaths every year, mainly in Asia and Africa [1]. Therefore, discovering an effective cure and a more cost-effective vaccine than the prevailing options is necessary to overcome this global public health problem.

Understanding the molecular functions of each RABV protein in detail is crucial for developing therapeutic strategies or avirulent live vaccines against rabies. The RABV genome encodes

five structural proteins: nucleoprotein, phosphoprotein, matrix protein, glycoprotein and large protein (N, P, M, G and L proteins, respectively). The N, P and L proteins form a ribonucleoprotein (RNP) complex together with the viral genomic RNA [2]. The M protein plays a key role in the recruitment of the RNP by host cell membranes and the budding of enveloped virus particles [3, 4]. The G protein forms projections from the surface of the viral envelope that bind to host cell receptors [5, 6]. To identify the viral proteins and amino acids responsible for the pathogenesis, we characterized two RABV strains: the Nishigahara strain, a virulent fixed strain with demonstrable lethality when inoculated intracerebrally to mice, and the Ni-CE

Received 04 December 2020; Accepted 09 April 2021; Published 23 April 2021

**Author affiliations:** <sup>1</sup>Transboundary Animal Diseases Research Center, Joint Faculty of Veterinary Medicine, Kagoshima University, 1-21-24 Korimoto, Kagoshima 890-0065, Japan; <sup>2</sup>Joint Graduate School of Veterinary Medicine, Kagoshima University, 1-21-24 Korimoto, Kagoshima 890-0065, Japan; <sup>3</sup>Laboratory of Zoonotic Diseases, Faculty of Applied Biological Sciences, Gifu University, 1-1 Yanagido, Gifu 501-1193, Japan; <sup>4</sup>Laboratory of Animal Hygiene, Joint Faculty of Veterinary Medicine, Kagoshima University, 1-21-24 Korimoto, Kagoshima 890-0065, Japan; <sup>5</sup>Joint Graduate School of Veterinary Sciences, Gifu University, 1-1 Yanagido, Gifu 501-1193, Japan.

\*Correspondence: Tatsunori Masatani, mstn@gifu-u.ac.jp

**Keywords:** apoptosis; caspases; matrix protein; phosphatidylserine; programmed cell death; rabies virus.

**Abbreviations:** ANOVA, analysis of variance; anti-N mAb, anti-rabies virus nucleoprotein monoclonal antibody; CPE, cytopathic effect; E-MEM, Eagle's minimum essential medium; G protein, glycoprotein; L protein, large protein; M95, amino acid at position 95 in the M protein; m.o.i., multiplicity of infection; M protein, matrix protein; N protein, nucleoprotein; PARP-1, poly(ADP-ribose) polymerase 1; PBS, phosphate-buffered saline; p.i., post-infection; P protein, phosphoprotein; PS, phosphatidylserine; RABV, rabies virus; RIPK1, Receptor-interacting serine/threonine-protein 1; RNP, ribonucleoprotein; SDS-PAGE, sodium dodecyl sulfate-polyacrylamide gel electrophoresis; Sts, staurosporine; TUNEL, terminal deoxynucleotidyl transferase-mediated dUTP nick-end labelling; VSV, vesicular stomatitis virus.

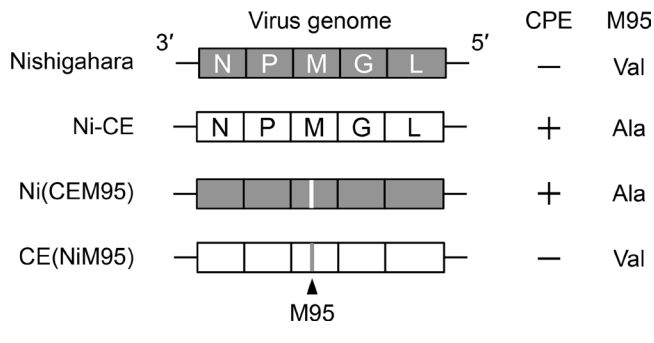


**Fig. 1.** Schematic diagram of the genome organization and CPE-inducing ability of the Nishigahara, Ni-CE and M95-mutated strains in NA cells. Grey and white lines represent M95 derived from the Nishigahara (Val) or the Ni-CE strain (Ala), respectively. -, low CPE in NA cells; +, high CPE in NA cells [9].

strain, a non-lethal offshoot of the Nishigahara strain obtained after 100 passages in chicken embryo fibroblast cells [7].

We previously reported that intracerebral inoculation of the CE(NiM95) strain, in which the Ala at position 95 in the M protein (M95) of Ni-CE was replaced with a Val from the M protein of the Nishigahara strain, was lethal in mice [8]. Moreover, we showed that M95 Ala is required to induce cell death because the Ni-CE strain, but not the Nishigahara or CE(NiM95) strain, induces a clear cytopathic effect (CPE) characterized by cell rounding, shrinkage and detachment in a mouse neuroblastoma cell line [9]. In general, RABV virulent strains do not induce prominent inflammation and cell death in the central nervous system, whereas fixed, non-lethal strains induce these effects, implying that the pathogenicity of RABV is inversely correlated with inflammation and cell death [10–12]. These previous studies suggest that the ability of M95 to induce cell death is correlated with the differences in the pathogenicity between the Nishigahara and Ni-CE strains; however, the intracellular signalling pathway involved in M95-induced cell death has not been elucidated.

We previously reported that CPE induced by the Ni-CE strain was accompanied by the apoptosis-like characteristics of cell death, displaying cell rounding, shrinkage and DNA fragmentation [9]. Apoptosis is a physiological process of cell death characterized by specific morphological and biochemical changes [13]. Caspases, a family of cysteine proteases, are prominent in apoptosis. Caspase-3 and -7 are well-known executioner caspases [14] that induce phosphatidylserine (PS) exposure, DNA fragmentation and cell shrinkage [15, 16]. Accordingly, apoptosis is defined as cell death caused by executioner caspases [17].

In this study, we aimed to elucidate the mechanisms by which M95 affects the cell death caused by RABV infection. We investigated cell death dynamics and apoptotic characteristics such as DNA fragmentation, activation of the executioner caspases, cell membrane disruption and PS exposure in human neuroblastoma cells infected with the Nishigahara, Ni-CE, or M95 mutant strains.

## METHODS

### Cells, viruses and reagents

Human SK-N-SH neuroblastoma cells and mouse NA neuroblastoma cells maintained in Eagle's minimum essential medium (E-MEM; FUJIFILM Wako Pure Chemical, Osaka, Japan) supplemented with 10% foetal calf serum, penicillin (100 U ml<sup>-1</sup>), streptomycin (100 µg ml<sup>-1</sup>) and amphotericin B (2.5 µg ml<sup>-1</sup>) were cultured at 37 °C in a humidified atmosphere with 5% CO<sub>2</sub>. The RABV strains targeted for evaluation were the Nishigahara, Ni-CE, CE(NiM95) and Ni(CEM95) strains; the latter strain was derived from the Nishigahara strain with a single substitution at M95 replacing valine (Nishigahara M95) with alanine (Ni-CE strain M95) (Fig. 1). Each strain was recovered from the relevant cloned cDNA as reported previously [7, 9, 18]. The fixed RABV strains CVS and ERA were also used as positive controls in this study. Stocks of all viruses

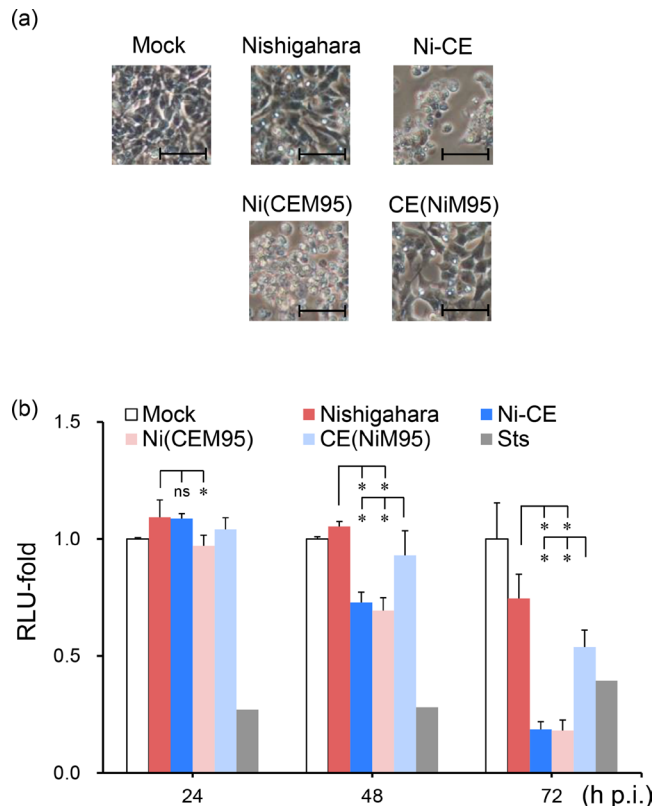


**Fig. 2.** Cell death induction by the Nishigahara, Ni-CE and M95-mutated strains in human neuroblastoma SK-N-SH cells. (a) CPE induction by the Nishigahara, Ni-CE and M95-mutated strains in SK-N-SH cells. Cells were infected with each strain (m.o.i.=1) and observed at 48 h post-infection (h p.i.) with a microscope. Scale bars represent 25 µm. (b) Viability of SK-N-SH cells infected with each strain at m.o.i.=3. After 24, 48 and 72 h p.i., cell viability was measured using a CellTiter-Glo assay kit. Cells treated with 1.0 µM staurosporine (Sts) for 4–6 h were used as positive controls. Luminescence is represented as the mean plus or minus the SD based on three wells; fold-changes in luminescence from the mock-infected sample are shown. The Student–Newman–Keuls test was used to determine statistical significance. \*, significant difference ( $P < 0.05$ ).

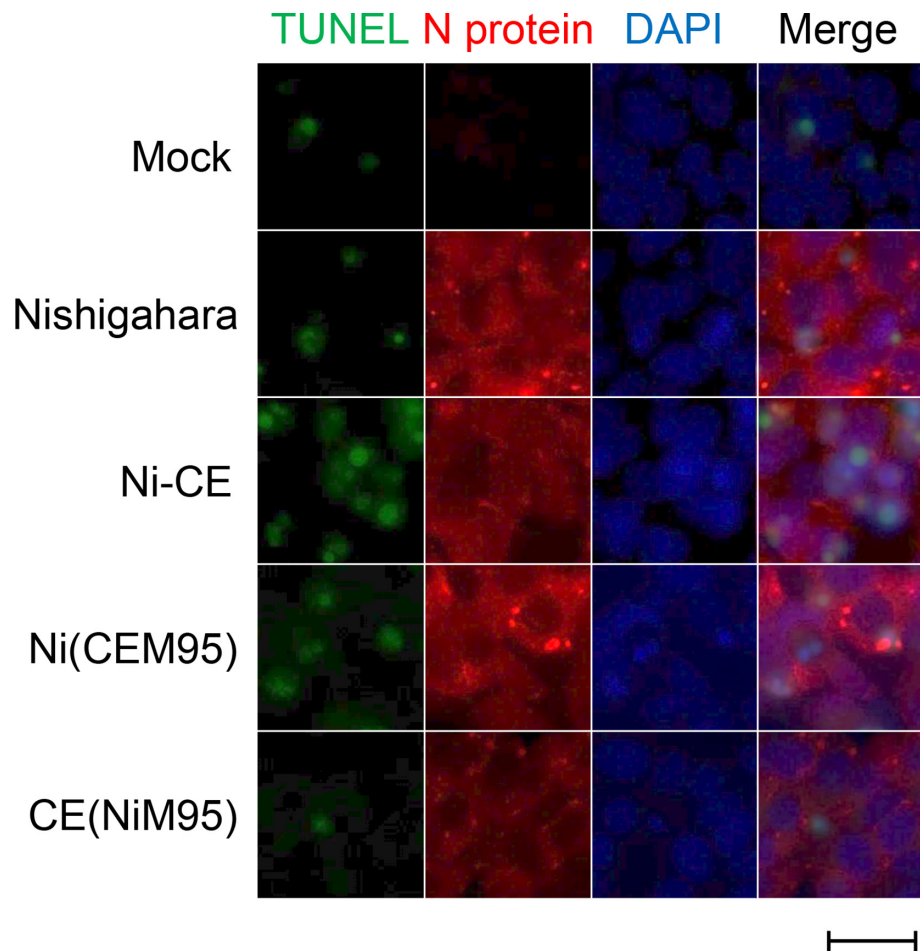


**Fig. 3.** Detection of apoptotic cells by TUNEL assay using SK-N-SH cells infected with the Nishigahara, Ni-CE, or M95-mutated strains. Cells were infected with each strain (m.o.i.=1). At 48 h p.i., apoptotic cells were detected by TUNEL staining. Green staining shows apoptotic cells (TUNEL-positive). Red staining shows cells infected with rabies virus (targeting N protein). Blue staining shows cell nuclei (DAPI). Scale bars represent 25  $\mu$ m.

were prepared in NA cells. Staurosporine (Sts; FUJIFILM Wako Pure Chemical) was used as an apoptosis inducer and Z-VAD-FMK (Peptide Institute, Ibaraki, Japan) was used as a caspase inhibitor.

### CPE observation

Monolayer SK-N-SH cultures grown in a 96-well plate (TPP, Trasadingen, Switzerland) were infected with each RABV strain at a multiplicity of infection (m.o.i.) of 1. Morphological changes in infected cells were observed with an inverted microscope (Eclipse Ti-S, Nikon, Tokyo, Japan) at 24, 48, and 72 h post-infection (p.i.).

### Cell viability assay

A CellTiter-Glo 2.0 Cell Viability Assay Kit (Promega, Madison, WI, USA) was used to measure ATP luminescence as an indicator of metabolically active cells. Briefly, SK-N-SH cells were cultured in a 96-well white plate (Thermo Fisher Scientific, Waltham, MA, USA) and

infected with each RABV strain (m.o.i.=3). At 24, 48 and 72 h p.i., equal volumes of the cell titre substrate buffer mixture and medium were added to each well. After shaking at room temperature for 1 min, luminescence was measured with a Glo-MAX Explorer Microplate Reader (Promega). Cells cultured with 1.0  $\mu$ M Sts for 4–6 h were used as positive controls.

### Terminal deoxynucleotidyl transferase-mediated dUTP nick-end labelling (TUNEL) assay

Apoptotic cells were detected by TUNEL assay using a MEBSTAIN Apoptosis TUNEL kit III (MBL, Aichi, Japan). Briefly, SK-N-SH cells grown on an eight-well chamber slide (SPL Life Sciences, Pocheon, Republic of Korea) were infected with each RABV strain (m.o.i.=1). At 48 h p.i., cells were fixed in phosphate-buffered saline (PBS) containing 4% paraformaldehyde (FUJIFILM Wako Pure Chemicals) for 30 min. Subsequently, the cells were permeabilized with 100% methanol at room temperature for 1 min. Before

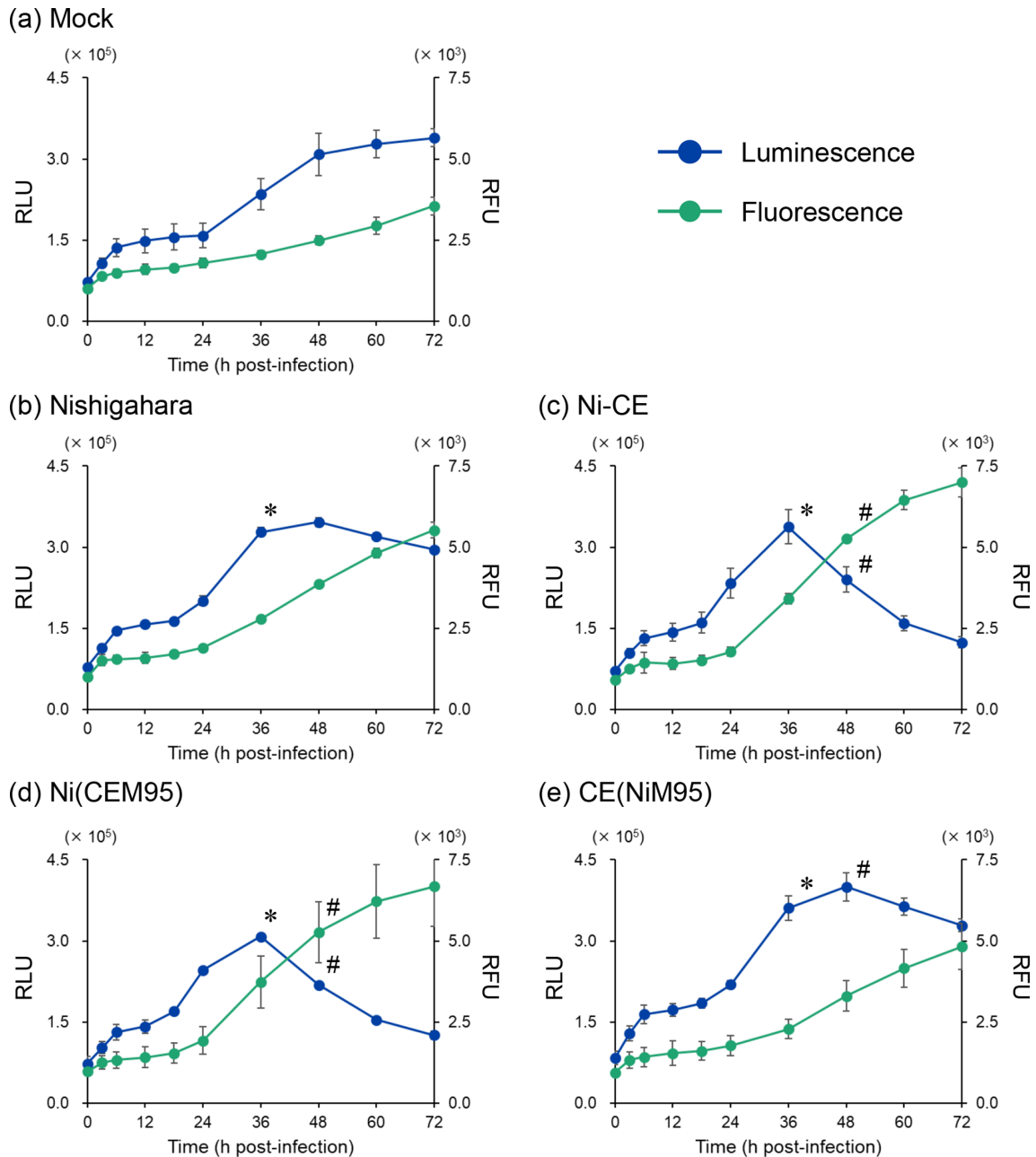


**Fig. 4.** Chronological analysis of PS exposure (luminescence) and cell membrane disruption (fluorescence). SK-N-SH cells were infected with mock (a) or the Nishigahara (b), Ni-CE (c), Ni(CEM95) (d), or CE(NiM95) (e) strain (m.o.i.=3). Luminescence and fluorescence are represented as the mean plus or minus SD based on three wells. The Student–Newman–Keuls test was used to determine statistical significance. \*,  $P < 0.05$  compared with mock-infected cells; #,  $P < 0.05$  compared with Nishigahara-infected cells.

TUNEL staining according to the manufacturer's instructions, the cells were incubated with an anti-RABV N protein mouse monoclonal antibody (anti-N mAb #13-27) [19] diluted in PBS at 37 °C for 30 min. After being washed five times with PBS, the slides were incubated with an Alexa Fluor 594-conjugated anti-mouse IgG secondary antibody (Invitrogen, Carlsbad, CA, USA) diluted in PBS at 4 °C overnight. After being washed five times with PBS, the nuclei were stained by ProLong Diamond Antifade Mountant with

DAPI (Invitrogen). Cells were examined using a BZ-X710 fluorescence microscope (Keyence, Osaka, Japan).

#### Real-time assessment of PS exposure and cell membrane disruption

Real-time assessment of PS exposure and cell membrane disruption as indicators of early and late apoptosis, respectively, was performed using a Real-Time-Glo Annexin V Apoptosis and

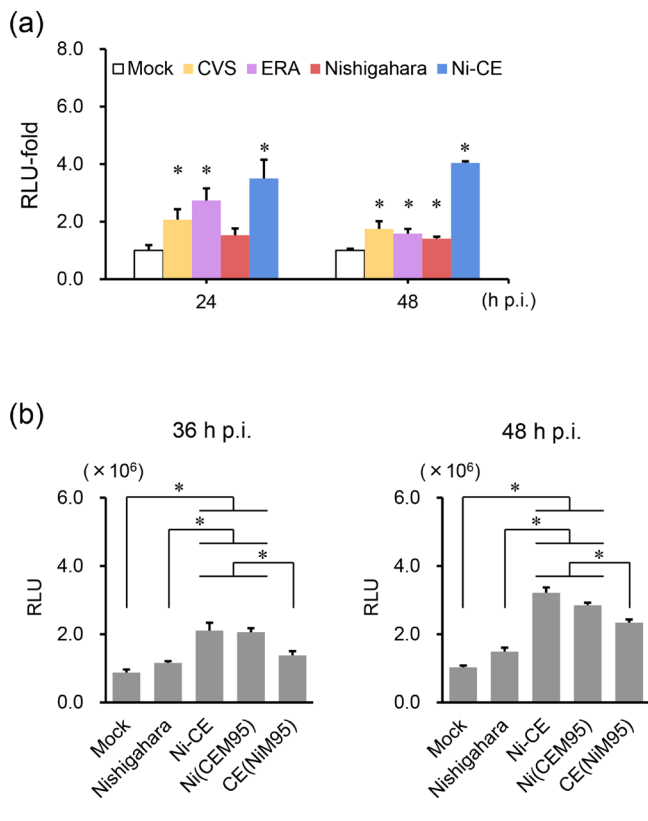


**Fig. 5.** Caspase-3/7 activities in RABV-infected SK-N-SH cells. (a) Caspase-3/7 activities in SK-N-SH cells infected with the CVS, ERA, Nishigahara and Ni-CE strains (m.o.i.=1) at 24 and 48 h p.i. Fold changes in luminescence from the mock-infected sample are shown. The Student–Newman–Keuls test was used to determine statistical significance. \*, significant difference versus mock-infected cells ( $P < 0.05$ ). (b) Caspase-3/7 activities in SK-N-SH cells infected with the Nishigahara, Ni-CE, Ni(CEM95) and CE(NiM95) strains at 36 and 48 h p.i. Luminescence is represented by the mean plus or minus the SD based on three wells. The Student–Newman–Keuls test was used to determine statistical significance. \*,  $P < 0.05$ .

Necrosis Assay (Promega) according to the manufacturer's instructions. Briefly, SK-N-SH cells were seeded into a 96-well white plate. After infection with each RABV strain (m.o.i.=3), cells were cultured in E-MEM containing the detection reagent, which had been prepared according to the manufacturer's instructions. Cells cultured in the same mixture containing 0.1  $\mu$ M Sts were used as positive controls. The luminescence and fluorescence of the cultured cells were measured chronologically to evaluate PS exposure and cell membrane disruption, respectively, at different time points using a Glo-MAX Explorer Microplate Reader.

### Caspase-3/7 activity assay

The caspase-3/7 activity of RABV-infected cells was detected using a Caspase-Glo 3/7 Assay (Promega). SK-N-SH cells were cultured in 96-well plates and infected with each RABV strain (m.o.i.=1). At 36 and 48 h p.i., the cells were lysed with Caspase-Glo buffer on ice for 10 min. Cells cultured with 1.0  $\mu$ M Sts for

4–6 h were used as positive controls. Cell lysates were transferred into a 96-well white plate and the corresponding caspase substrate dissolved in Caspase-Glo buffer was added. After shaking at room temperature for 1 min, caspase-3/7 activity was measured as luminescence using a Glo-MAX Explorer Microplate Reader.

### Western blotting

SK-N-SH cells infected with each RABV strain (m.o.i.=1) were lysed at 24 h p.i. using RIPA buffer [50 mM Tris-HCl (pH 7.5), 150 mM NaCl, 1 mM EDTA, 1% NP-40, 0.5% sodium deoxycholate] including a protease inhibitor cocktail (Nacalai Tesque, Kyoto, Japan). After incubation on ice for 15 min, the cell lysates were centrifuged (12000 g, 10 min, 4 °C), and the collected supernatants were mixed with an equal volume of 2 $\times$  sodium dodecyl sulfate/polyacrylamide gel electrophoresis (SDS-PAGE) sample buffer [125 mM Tris/HCl (pH 6.8), 4% SDS, 20% (w/v) glycerol, 0.01% bromophenol blue, 10% (v/v) 2-mercaptoethanol]. After incubation at 95 °C for 5 min, proteins in the samples were separated by 10% SDS-PAGE and then transferred onto Immobilon-P membranes (Merck Millipore, Burlington, MA, USA). After blocking with PBS containing 5% skim milk (FUJIFILM Wako Pure Chemicals) and 0.1% Tween-20 (FUJIFILM Wako Pure Chemicals), membranes were incubated at 4 °C overnight with anti-poly (ADP-ribose) polymerase 1 (PARP-1) rabbit monoclonal antibody (#9542, Cell Signaling, Danvers, MA, USA), anti-N mAb #13–27, or anti-tubulin mouse monoclonal antibody (T5168; Sigma Aldrich, St Louis, MO, USA) diluted in PBS containing 1% skim milk and 0.1% Tween-20. After washing with PBS containing 0.1% Tween-20, the membranes were incubated at 37 °C for 1 h with horseradish peroxidase-conjugated anti-mouse IgG (P0260, Dako, Glostrup, Denmark) or anti-rabbit IgG (P0448, Dako) as the secondary antibody. Protein bands were visualized using ECL Prime Western Blotting Detection Reagent (GE Healthcare, Chicago, IL, USA), and images were acquired using ImageQuant LAS 500 (GE Healthcare).

### Statistical analysis

Statistically significant differences between two groups were analysed using Student's *t*-test and among multiple groups were analysed using one-way analysis of variance (ANOVA), followed by the Student–Newman–Keuls test. A *P*-value of <0.05 was considered statistically significant.

## RESULTS

### Ni-CE and Ni(CEM95) strains induced stronger CPE and reduced cell viability in human neuroblastoma cells

To investigate whether the cell death induced by Ni-CE infection observed in mouse neuroblastoma NA cells [9] also occurred in other cell lines, we inoculated Nishigahara, Ni-CE and M95 mutants [CE(NiM95) and Ni(CEM95)] into human SK-N-SH neuroblastoma cells. We observed a stronger CPE in SK-N-SH cells infected with the Ni-CE and Ni(CEM95) strains than in those infected with Nishigahara

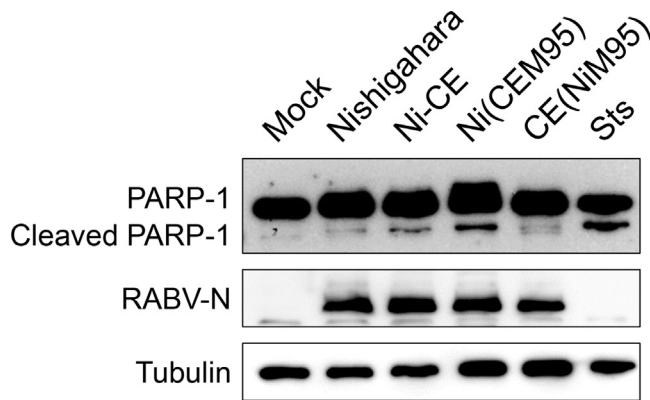


**Fig. 6.** Western blot analysis of PARP-1 cleavage. SK-N-SH cells were infected with each RABV strain (m.o.i.=1) and lysed at 24 h p.i. Cells treated with 1.0  $\mu$ M Sts for 4–6 h were used as positive controls. Proteins were detected with antibodies against PARP-1 and the RABV N protein (RABV-N). Tubulin was used as a loading control.

and CE(NiM95) strains at 48 h p.i. (Fig. 2a); specifically, cells infected with the Ni-CE and Ni(CEM95) strains were more rounded, shrunken and detached, resembling the response previously reported in NA cells. Furthermore, to determine whether CPE is related to cell death, we investigated cell viability by measuring ATP luminescence. SK-N-SH cells infected with the Ni-CE and Ni(CEM95) strains showed lower luminescence than cells infected with the Nishigahara and CE(NiM95) strains (Fig. 2b), demonstrating that the Ni-CE and Ni(CEM95) strains induced cell death more strongly. These results indicate that the M95 position is also related to the human SK-N-SH cell death induced by Ni-CE infection.

### M95-related cell death also results in DNA fragmentation

A TUNEL assay to detect DNA fragmentation, a characteristic of apoptosis, was performed on SK-N-SH cells infected with each RABV strain. A greater proportion of TUNEL-positive cells were detected among SK-N-SH cells infected with the Ni-CE and Ni(CEM95) strains than among those infected with the Nishigahara and CE(NiM95) strains (Fig. 3). This result suggests that DNA fragmentation occurs during the process of cell death induced by Ni-CE infection.

### M95-related cell death is involved in cell membrane disruption

To investigate the relationship between cell death induced by Ni-CE infection and the host cell membrane, we detected PS exposure and cell membrane disruption in real-time using SK-N-SH cells infected with each RABV strain. Luminescence and fluorescence (representing PS exposure and cell membrane disruption, respectively) were measured at different time points in the infected cells. Both Ni-CE- and Nishigahara-infected cells showed higher luminescence than mock-infected cells between 18 and 36 h p.i., with comparable levels of luminescence (Fig. 4a–e). Notably, after 36 h p.i.,

luminescence decreased dramatically in Ni-CE-infected cells but not in Nishigahara-infected cells. In contrast, fluorescence levels were higher in Ni-CE-infected cells than in Nishigahara-infected cells between 18 and 72 h p.i. These results suggest that the Ni-CE strain induced cell membrane disruption and cell death through PS exposure, whereas Nishigahara strains did not induce cell membrane disruption despite PS exposure. Notably, Ni(CEM95)-infected and CE(NiM95)-infected cells showed the same dynamics of luminescence and fluorescence as those of Ni-CE-infected and Nishigahara-infected cells, respectively (Fig. 4d, e). These results indicate that M95 is strongly related to cell membrane disruption but not to PS exposure.

### Activation of caspase-3/7 is involved in M95-related cell death for SK-N-SH cells

Apoptosis is induced by executioner caspases, mainly caspase-3, according to the definition of the Nomenclature Committee on Cell Death [17]. Thus, we examined the activity of executioner caspases in SK-N-SH cells infected with each strain to clarify whether cell death induced by Ni-CE infection is associated with apoptosis. We demonstrated that the Ni-CE strain induced caspase-3/7 activity, in a similar manner to the positive control RABV strains (CVS and ERA) [20, 21], and this induced activity was significantly greater than that seen with mock infection or the Nishigahara strain in SK-N-SH cells (Fig. 5a). Notably, the Ni-CE and Ni(CEM95) strains induced higher caspase-3/7 activity than either mock infection or the Nishigahara or CE(NiM95) strain (Fig. 5b). These results indicate that the cell death induced by Ni-CE infection is associated with the activation of executioner caspases.

### PARP-1 cleavage is involved in M95-related cell death

Cleavage of PARP-1 by caspases is considered to be a hallmark of apoptosis [22]. Thus, we investigated PARP-1 cleavage in SK-N-SH cells infected with each strain. Distinct PARP-1 cleavage was detected in cells infected with the Ni-CE and Ni(CEM95) strains and cells treated with Sts. However, PARP-1 cleavage was less pronounced in cells infected with the Nishigahara and CE(NiM95) strains than in those infected with the Ni-CE and Ni(CEM95) strains (Fig. 6). This result indicates that PARP-1 cleavage is involved in cell death induced by Ni-CE infection.

### Cell death induced by Ni-CE infection is also related to the caspase-independent pathway

To investigate whether the cell death induced by Ni-CE infection depends on canonical caspase-dependent apoptosis, we investigated the caspase-3/7 activity, PARP-1 cleavage and cell viability of RABV-infected cells in the presence of the caspase inhibitor Z-VAD-FMK (Fig. 7). We demonstrated that Z-VAD-FMK significantly reduced caspase-3/7 activity in SK-N-SH cells infected with the Ni-CE and Ni(CEM95) strains (Fig. 7a). Moreover, PARP-1 cleavage was partially recovered in cells infected with each RABV strain by treatment with Z-VAD-FMK (Fig. 7b). These results suggest that

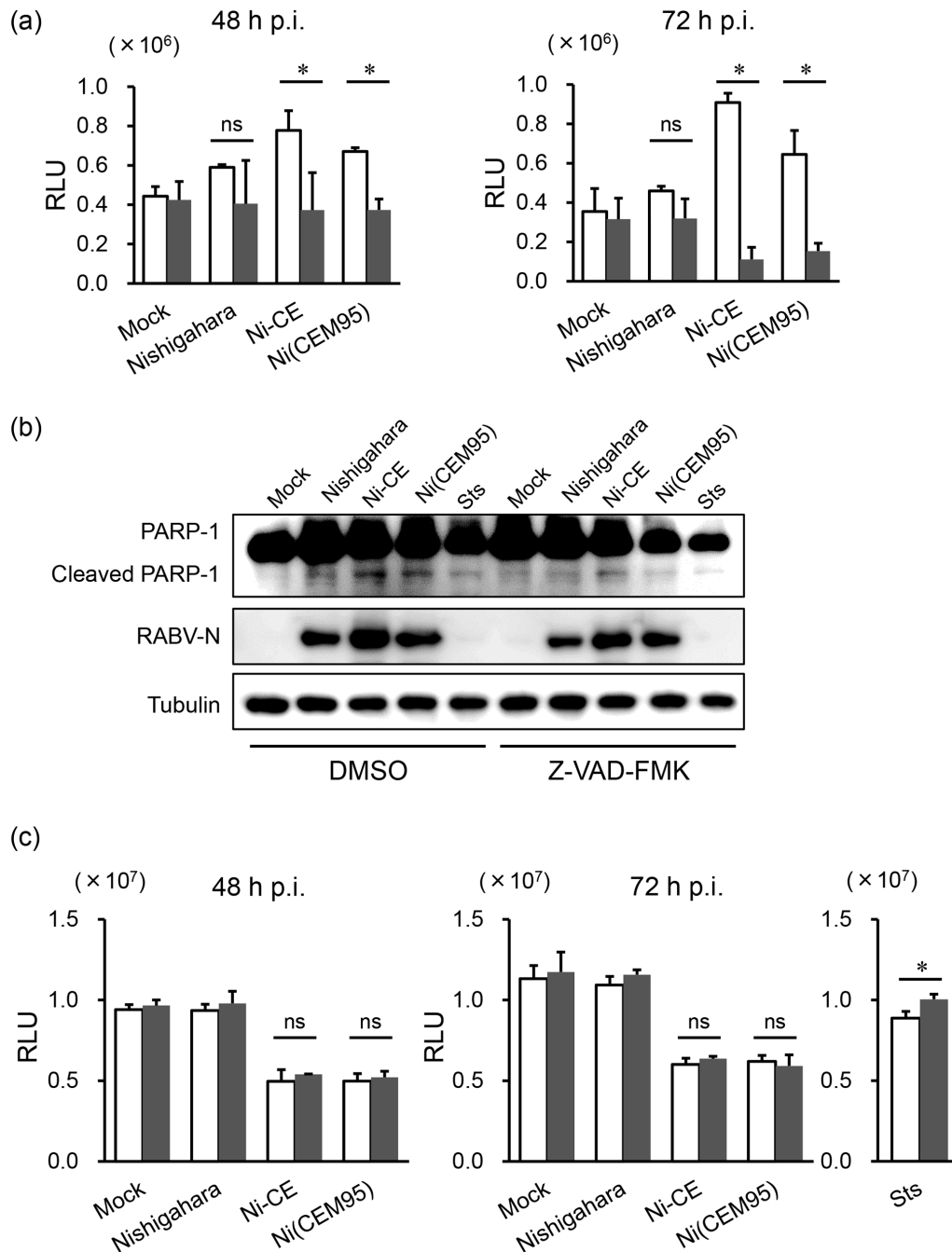


**Fig. 7.** Effect of the caspase inhibitor Z-VAD-FMK on caspase-3/7 activity, cell viability and PARP-1 cleavage on SK-N-SH cells infected with the Nishigahara, Ni-CE and Ni(CEM95) strains. (a) Effects of the caspase inhibitor Z-VAD-FMK on caspase-3/7 activity in SK-N-SH cells infected with the Nishigahara, Ni-CE and Ni(CEM95) strains (m.o.i.=1). DMSO (white bars) or Z-VAD-FMK (20  $\mu$ M; grey bars) was treated after RABV infection. After 48 and 72 h p.i., caspase-3/7 activity was measured. Luminescence is represented as the mean plus or minus the SD based on three wells. The Student–Newman–Keuls test was used to determine statistical significance. \*, significant difference ( $P < 0.05$ ). (b) SK-N-SH cells were infected with each RABV strain (m.o.i.=1). Cells were treated with DMSO or Z-VAD-FMK (20  $\mu$ M) after RABV infection and lysed at 48 h p.i. Cells treated with 1.0  $\mu$ M Sts for 4–6 h were used as positive controls. Proteins were detected with antibodies against PARP-1 and the RABV N protein (RABV-N). Tubulin was used as a loading control. (c) Effect of Z-VAD-FMK treatment on the viability of SK-N-SH cells infected with each RABV strain (m.o.i.=1). Cells were treated with DMSO (white bars) or Z-VAD-FMK (20  $\mu$ M; grey bars) after RABV infection. At 48 and 72 h p.i., cell viability was measured using a Cell Titer Glo assay kit. Cells treated with 0.1  $\mu$ M staurosporine (Sts) for 72 h were used as positive controls. Luminescence is represented as the mean plus or minus the SD based on three wells. The Student–Newman–Keuls test was used to determine statistical significance. \*, significant difference ( $P < 0.05$ ).

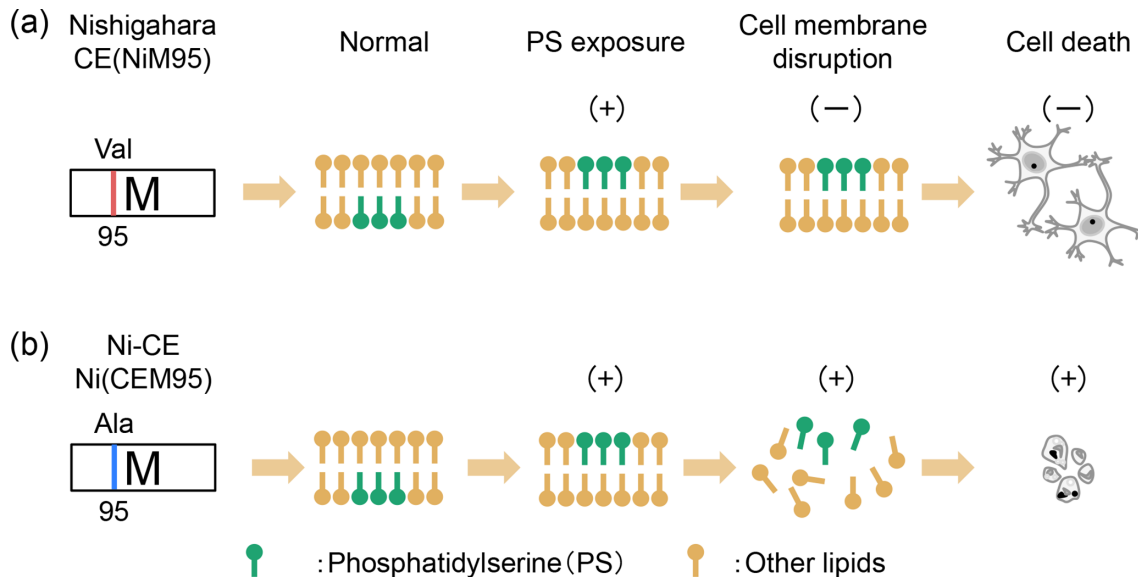


**Fig. 8.** Summary of M95-related cell membrane dynamics in SK-N-SH cells infected with RABV. (a) The Nishigahara or CE(NiM95) strain does not induce cell membrane disruption despite PS exposure. (b) The Ni-CE or Ni(CEM95) strain induces cell membrane disruption through PS exposure.

the mechanism of cell death induced by Ni-CE infection is related to executioner caspases in SK-N-SH cells. However, despite the fact that Z-VAD-FMK treatment at the same concentration inhibited the activity of caspase-3/7, there was no recovery of viable cells by Z-VAD-FMK treatment in cells infected with each virus strain (Fig. 7c). These results suggest that the cell death induced by Ni-CE infection depends on a caspase-independent pathway as well as caspase-dependent canonical apoptosis.

## DISCUSSION

Previous studies have shown that attenuated RABV strains induce cell death both *in vitro* and *in vivo*, whereas virulent RABV strains have shown less pronounced effects [11, 20, 23, 24]. Therefore, the suppression of cell death induction is considered to be one of the mechanisms of RABV pathogenesis. However, the exact mechanism underlying cell death induced by attenuated RABV remains unknown. In this study, using the Nishigahara and Ni-CE strains and their M95-mutant viruses, we demonstrated that the amino acid at position 95 of the RABV M protein plays a crucial role in cell membrane disruption, but not in PS exposure. Moreover, we showed that cell death induced by Ni-CE infection was not only associated with the caspase-3/7 pathway, the major executioner caspases in apoptosis, but also with the caspase-independent pathway.

In this study, when human SK-N-SH cells were inoculated with each RABV strain, the cells infected with the Ni-CE and Ni(CEM95) strains showed significant CPE and cell death and prominent DNA fragmentation, whereas those infected with the Nishigahara and CE(NiM95) strains induced low

CPE or DNA fragmentation (Figs 2 and 3). These results were similar to those of Mita *et al.* [9] for NA cells derived from mouse neuroblastomas. This suggests that the M95 mutation is involved in cell death in neuroblastoma cells from different animal species.

A recent study has also shown that the RABV M protein is a cytopathic determinant [21] and that the amino acids at positions 67–79 of the M protein of the CVS-11 strain, a fixed RABV strain, are related to cell death characterized by DNA fragmentation, PARP-1 cleavage, and caspase-3 activation in mouse neuroblastoma N2a cells [21]. Here, we found that the Ni-CE strain also induced similar DNA fragmentation, PARP-1 cleavage and caspase-3/7 activation to those induced by the CVS-11 strain in human neuroblastoma SK-N-SH cells. Notably, it has been shown that the CVS-11 strain also activates both caspase-dependent and caspase-independent cell death pathways [24]. These findings suggest that RABV-induced cell death may be caused by a common mechanism among multiple strains, although there are differences in the amino acid regions that determine it.

Although all strains used in this study induced PS exposure on the cell membrane, the Ni-CE and Ni(CEM95) strains, but not the Nishigahara and CE(NiM95) strains, dramatically induced cell membrane disruption (Fig. 4), strongly suggesting that M95 is related to cell membrane disruption. Thus, the M protein with Ala at M95 may induce cell membrane disruption followed by PS exposure, whereas the M protein with Val at M95 does not induce cell membrane disruption despite the occurrence of PS exposure (Fig. 8). Generally, cell membrane disruption occurs after PS exposure [25]. Three major mechanisms of PS exposure have

been described thus far: (1) Ca<sup>2+</sup>-mediated activation of TMEM16F; (2) caspase-mediated activation of Xkr8; and (3) caspase-mediated inactivation of the 'flippase' complex, ATP11c and CDC50a [26–29]. In this study, we showed that cell death induced by Ni-CE infection was caspase-dependent in SK-N-SH cells, suggesting the involvement of either the Xkr8 or flippase complex mechanism. However, we found that SK-N-SH cells infected with the Ni-CE and Ni(CEM95) strains induced cell membrane disruption followed by PS exposure in the presence of Z-VAD-FMK (data not shown). Therefore, Ca<sup>2+</sup>-mediated activation of TMEM16F, which is known as a caspase-independent phenomenon, may be associated with the M95-related cell death mechanism. Additionally, galectin-1, a  $\beta$ -galactoside-binding lectin, has been reported to induce PS exposure in neutrophils without altering cell viability [30]. Therefore, the Ni-CE and Ni(CEM95) strains may also induce PS exposure by activating galectin-1. Further molecular studies are needed to elucidate the mechanism of cell death following PS exposure involving M95.

In the present study, we showed that the PARP-1 cleavage during M95-related cell death was partially recovered by the caspase inhibitor, Z-VAD-FMK. PARP-1 is an intracellular protein that detects and repairs DNA breaks [31] and is mostly cleaved by activated caspase-3/7 [32, 33]. However, PARP-1 cleavage is triggered by both caspase-dependent and -independent pathways. Masdehors *et al.* [34] reported that PARP-1 cleavage may be regulated by a ubiquitin-associated 'N-end rule pathway' in a caspase-independent manner. In contrast, Yang *et al.* [35] demonstrated that transforming growth factor- $\beta$ , a cytokine involved in various physiological processes, induces PARP-1 cleavage in the presence of a caspase inhibitor. Thus, PARP-1 cleavage occurring during Ni-CE infection-induced cell death may be associated with both caspase-dependent and caspase-independent signalling.

Here, we demonstrated that the Ni-CE strain induced cell death regardless of the presence of Z-VAD-FMK. Thus, caspase-independent programmed cell death mechanisms may also be associated with cell death induced by Ni-CE infection. New types of programmed cell death have recently been discovered [17], some of which are caspase-independent and induce antiviral immune responses [36–38]. For instance, the M protein of the vesicular stomatitis virus (VSV), a member of the family *Rhabdoviridae*, is involved in the novel cell death systems, necroptosis and parthanatos [37, 39]. Necroptosis is a newly discovered type of programmed cell death that is morphologically necrotic and caspase-independent. Receptor-interacting serine/threonine-protein 1 (RIPK1), a key signalling molecule in necroptosis [17], is upregulated in cells transfected with the VSV M protein [37]. In contrast, the VSV M protein may also induce parthanatos, which is another programmed cell death pathway that causes DNA fragmentation by PARP hyperactivation and apoptosis-inducing factor activation [39, 40]. We have not found any homologous amino acid regions between the VSV and RABV M proteins that might be associated with these novel forms of cell death. However, the question of whether the RABV M protein activates these systems requires further investigation.

In conclusion, we found that cell death induced by Ni-CE infection is characterized by PS exposure following cell membrane disruption and is related to both caspase-dependent and caspase-independent pathways in SK-N-SH cells. The mechanisms by which a single amino acid change is involved in cell death remains unclear and the details of caspase-dependent and caspase-independent signalling are still unknown. We believe that elucidation of the mechanism of RABV-induced cell death would be a great advance in our understanding of the pathogenicity of this virus.

#### Funding information

This study was supported partially by the Japan Society for the Promotion of Science (JSPS) Grant-Aid for Scientific Research (KAKENHI: grant no. 17K08083) and GSK Japan Research Grant 2020 for T. M.

#### Acknowledgements

We would like to thank Editage (<https://www.editage.jp/>) and Mr Henry Smith (Joint Graduate School of Veterinary Medicine, Kagoshima University) for language assistance in the drafting of this manuscript.

#### Conflicts of interest

The authors declare that there are no conflicts of interest.

#### References

- Hampson K, Coudeville L, Lembo T, Sambo M, Kieffer A. Estimating the global burden of endemic canine rabies. *PLoS Negl Trop Dis* 2015;9:1–20.
- Chenik M, Chebli K, Gaudin Y, Blondel D. In vivo interaction of rabies virus phosphoprotein (P) and nucleoprotein (N): existence of two N-binding sites on P protein. *J Gen Virol* 1994;75:2889–2896.
- Finke S, Conzelmann KK. Dissociation of rabies virus matrix protein functions in regulation of viral RNA synthesis and virus assembly. *J Virol* 2003;77:12074–12082.
- Wirblich C, Tan GS, Papaneri A, Godlewski PJ, Orenstein JM *et al.* PPEY motif within the rabies virus (RV) matrix protein is essential for efficient virion release and RV pathogenicity. *J Virol* 2008;82:9730–9738.
- Dietzschold B, Li J, Faber M, Schnell M. Concepts in the pathogenesis of rabies. *Future Virol* 2008;3:481–490.
- Finke S, Conzelmann KK. Replication strategies of rabies virus. *Virus Res* 2005;111:120–131.
- Shimizu K, Ito N, Mita T, Yamada K, Hosokawa-Muto J *et al.* Involvement of nucleoprotein, phosphoprotein, and matrix protein genes of rabies virus in virulence for adult mice. *Virus Res* 2007;123:154–160.
- Ito N, Mita T, Shimizu K, Ito Y, Masatani T *et al.* Amino acid substitution at position 95 in rabies virus matrix protein affects viral pathogenicity. *J Vet Med Sci* 2011;73:1363–1366.
- Mita T, Shimizu K, Ito N, Yamada K, Ito Y *et al.* Amino acid at position 95 of the matrix protein is a cytopathic determinant of rabies virus. *Virus Res* 2008;137:33–39.
- Jackson AC, Rasalingam P, Welis SC. Comparative pathogenesis of recombinant rabies vaccine strain SAD-L16 and SAD-D29 with replacement of Arg333 in the glycoprotein after peripheral inoculation of neonatal mice: less neurovirulent strain is a stronger inducer of neuronal apoptosis. *Acta Neuropathol* 2006;111:372–378.
- Morimoto K, Hooper DC, Spitsin S, Koprowski H, Dietzschold B. Pathogenicity of different rabies virus variants inversely correlates with apoptosis and rabies virus glycoprotein expression in infected primary neuron cultures. *J Virol* 1999;73:510–518.
- Suja MS, Mahadevan A, Madhusudana SN, Shankar SK. Role of apoptosis in rabies viral encephalitis: a comparative study in mice, canine, and human brain with a review of literature. *Patholog Res Int* 2011;2011:1–13.
- Ashkenazi A, Dixit VM. Death receptors: signaling and modulation. *Science* 1998;281:1305–1308.

14. Julien O, Wells JA. Caspases and their substrates. *Cell Death Differ* 2017;24:1380–1389.
15. Larsen BD, Sørensen CS. The caspase-activated DNase: apoptosis and beyond. *FEBS J* 2017;284:1160–1170.
16. Suzuki J, Imanishi E, Nagata S. Xkr8 phospholipid scrambling complex in apoptotic phosphatidylserine exposure. *Proc Natl Acad Sci U S A* 2016;113:9509–9514.
17. Galluzzi L, Vitale I, Aaronson SA, Abrams JM, Adam D et al. Molecular mechanisms of cell death: recommendations of the nomenclature Committee on cell death 2018. *Cell Death Differ* 2018;25:486–541.
18. Yamada K, Ito N, Takayama-Ito M, Sugiyama M, Minamoto N. Multi-genic relation to the attenuation of rabies virus. *Microbiol Immunol* 2006;50:25–32.
19. Minamoto N, Tanaka H, Hishida M, Goto H, Ito H et al. Linear and conformation-dependent antigenic sites on the nucleoprotein of rabies virus. *Microbiol Immunol* 1994;38:449–455.
20. Thoulouze M, Lafage M, Montano-Hirose JA, Lafon M. Rabies virus infects mouse and human lymphocytes and induces apoptosis. *J Virol* 1997;71:20:7372–7380.
21. Zan J, Liu J, Zhou JW, Wang HL, Mo K-K et al. Rabies virus matrix protein induces apoptosis by targeting mitochondria. *Exp Cell Res* 2016;347:83–94.
22. Chaitanya GV, Steven AJ, Babu PP. Parp-1 cleavage fragments: signatures of cell-death proteases in neurodegeneration. *Cell Commun Signal* 2010;8:31.
23. Yan X, Prośniak M, Curtis MT, Weiss ML, Faber M et al. Silver-haired bat rabies virus variant does not induce apoptosis in the brain of experimentally infected mice. *J Neurovirol* 2001;7:518–527.
24. Sarmiento L, Tseggai T, Dhingra V, Fu ZF. Rabies virus-induced apoptosis involves caspase-dependent and caspase-independent pathways. *Virus Res* 2006;121:144–151.
25. Silva MT, do Vale A, dos Santos NMN. Secondary necrosis in multicellular animals: an outcome of apoptosis with pathogenic implications. *Apoptosis* 2008;13:463–482.
26. Segawa K, Kurata S, Yanagihashi Y, Brummelkamp TR, Matsuda F et al. Caspase-Mediated cleavage of phospholipid flippase for apoptotic phosphatidylserine exposure. *Science* 2014;344:1164–1168.
27. Suzuki J, Umeda M, Sims PJ, Nagata S. Calcium-Dependent phospholipid scrambling by TMEM16F. *Nature* 2010;468:834–838.
28. Suzuki J, Denning DP, Imanishi E, Horvitz HR, Nagata S. Xk-Related protein 8 and CED-8 promote phosphatidylserine exposure in apoptotic cells. *Science* 2013a;341:403–406.
29. Suzuki J, Fujii T, Imao T, Ishihara K, Kuba H et al. Calcium-Dependent phospholipid scramblase activity of TMEM16 protein family members. *J Biol Chem* 2013b;288:13305–13316.
30. Stowell SR, Karmakar S, Arthur CM, Ju T, Rodrigues LC et al. Galectin-1 induces reversible phosphatidylserine exposure at the plasma membrane. *Mol Biol Cell* 2009;20:1408–1418.
31. Ivana Scovassi A, Diederich M. Modulation of poly(ADP-ribosylation) in apoptotic cells. *Biochem Pharmacol* 2004;68:1041–1047.
32. Salvesen GS, Dixit VM. Caspases: intracellular signaling by proteolysis. *Cell* 1997;91:443–446.
33. Boucher D, Blais V, Denault JB. Caspase-7 uses an exosite to promote poly(ADP ribose) polymerase 1 proteolysis. *Proc Natl Acad Sci U S A* 2012;109:5669–5674.
34. Masdehors P, Glaisner S, Maciorowski Z, Magdelénat H, Delic J. Ubiquitin-dependent protein processing controls radiation-induced apoptosis through the N-end rule pathway. *Exp Cell Res* 2000;257:48–57.
35. Yang Y, Zhao S, Song J. Caspase-dependent apoptosis and -independent poly(ADP-ribose) polymerase cleavage induced by transforming growth factor beta1. *Int J Biochem Cell Biol* 2004;36:223–234.
36. Upton JW, Shubina M, Balachandran S. RIPK3-driven cell death during virus infections. *Immunol Rev* 2017;277:90–101.
37. Douzandegan Y, Tahamtan A, Gray Z, Nikoo HR, Tabarraei A et al. Cell death mechanisms in esophageal squamous cell carcinoma induced by vesicular stomatitis virus matrix protein. *Osong Public Heal Res Perspect* 2019;10:246–252.
38. Tang D, Kang R, Berghe TV, Vandenebeele P, Kroemer G. The molecular machinery of regulated cell death. *Cell Res* 2019;29:347–364.
39. Gadaleta P, Perfetti X, Mersich S, Coulombié F. Early activation of the mitochondrial apoptotic pathway in vesicular stomatitis virus-infected cells. *Virus Res* 2005;109:65–69.
40. Wang Y, Kim NS, Haince JF, Kang HC, David KK et al. Poly(ADP-ribose) (PAR) binding to apoptosis-inducing factor is critical for PAR polymerase-1-dependent cell death (parthanatos). *Sci Signal* 2011;4:ra20.

### Five reasons to publish your next article with a Microbiology Society journal

1. The Microbiology Society is a not-for-profit organization.
2. We offer fast and rigorous peer review – average time to first decision is 4–6 weeks.
3. Our journals have a global readership with subscriptions held in research institutions around the world.
4. 80% of our authors rate our submission process as 'excellent' or 'very good'.
5. Your article will be published on an interactive journal platform with advanced metrics.

Find out more and submit your article at [microbiologyresearch.org](https://microbiologyresearch.org).